EXPERIMENTAL STUDY ON SEISMIC BEHAVIOR OF REINFORCED CONCRETE SUBASSEMBLAGES WITH SLITTED SPANDREL WALLS

T. Ichinose (I), H. Aoyama (II) and Y. Kai (III)
Presenting Author: T. Ichinose

ABSTRACT

Nonstructural monolithic spandrel walls in the reinforced concrete frames shorten the deformable length of columns, where shear failure has been often observed after earthquakes. In order to avoid such failure and lead the entire frame to the weak girder collapse type, a slit was introduced between the column and the spandrel. Beam-column subassemblages with slitted spandrel walls were tested to study the effect of slits upon the beam end rotational capacity and the energy dissipating capacity.

INTRODUCTION

One advantage of reinforced concrete construction is its ability to build various elements of the structure monolithically. In Japan, this advantage is greatly emphasized from the architectural point of view, and it is a quite common practice for Japanese constructors to place concrete simultaneously into structural members as well as architectural elements, such as spandrels, parapets, cornices, lintels, studs, canopies and balconies. This practice creates a favourable condition for reinforced concrete in the economic competition.

On the other hand, architectural concrete often causes unfavourable interaction with the structural concrete, particularly under seismic excitation. The most remarkable is the shear failure of reinforced concrete "captive" columns shortened by the monolithic spandrel walls(1). From the structural designer's viewpoint, it is clear that such nonstructural elements should not be introduced into the structure unless they are duely considered in the process of structural analysis, proportioning and detailing. However, in the current Japanese construction industry, the complete elimination of architectural concrete might lead to the economic suicide of reinforced concrete construction.

In an effort to reconcile architectural concrete with the structure, it is often recommended that spandrel walls be separated from the columns while attached monolithically to the girders(2). It can be achieved by introducing slits between columns and spandrel walls, rendering columns more flexibility. A question arises as to whether such "slitted" girders can develop plastic hinges, leading the entire frame to the weak girder type collapse mechanism. The objective of this study is to investigate the behavior of reinforced concrete beam-column subassemblages having slitted spandrel walls under reversal of simulated seismic loading, especially the effect of vertical slits upon the beam end rotational capacity, energy dissipation capacity within the limited slit width, effect of the contact of the spandrel walls to the column face at a large displacement, and overall deformation pattern of the beams

(I) Research Associate, Nagoya Institute of Technology, Nagoya, Japan
(II) Professor, The University of Tokyo, Tokyo, Japan
(III) Nuclear Power Department, Shimizu Construction Co. Ltd., Tokyo, Japan

with spandrel walls.

TEST SPECIMENS

The test specimens are half-scale models of a second floor spandrel beam-column subassemblage of a four-story school building. Six specimens are tested. Reinforcement details and principal parameters of the specimens are shown in Fig.1 and Table 1. The numbers and the characters after "SW" indicate the approximate width of the slit in cm and features of the specimens, respectively. The slit width of SW00 in zero (monolithic spandrel), the slit width of SW10 is 10cm, and those of the other specimens are approximately 1cm. In the specimen SWS1, the depth of the column is smaller and the beam bar diameter is larger than those of the other specimens. The beam tensile reinforcement ratio of the specimens SWU1 and SWS1 is unbalanced, i.e., the top reinforcement is twice of the bottom reinforcement. the horizontal reinforcements in the spandrel of the specimens SW00 and SW01 are anchored in the connecting columns, whereas those of the other specimens are terminated within the spandrel. Mechanical properties of the materials are shown in Tables 2 and 3. All specimens including SW00 were designed so that the beams yielded prior to column yielding and to shear failure in the beams and columns.

The top and bottom of a column were supported by a vertical roller and a hinge as shown in Fig2(a). Constant axial load, P = 24t (P/bDF_c = 0.07 to 0.11), was applied at the top of the column. The deflection at the two beam ends were moved vertically by the same amplitude, but in the opposite direction, so that an equivalent interstory displacement, delta in Fig2(b), followed the given displacement schedule in Fig3.

STORY SHEAR - STORY DISPLACEMENT RELATIONSHIP

The story shear-displacement relationships are shown in Fig4. The yield story shear is defined as the column shear at the flexural yielding of the two beams. Calculated yield shear values are indicated by broken lines in Fig4. Tensile and compressive stress of horizontal spandrel reinforcement was considered to calculate the yield strength of SW01. Observed yield story shears were close to the calculated values.

The strength degradation of SW00 was mainly due to the crushing and spalling of the spandrel concrete. The strength degradation of SW01 was due to the bond deterioration of the spandrel reinforcement anchored into the column. Prominent "pinching" was observed in the hysteresis loops of SWS1, because the shear deformation and the bond deterioration were large in the joint. The hysteresis loops of SW01 and SW10 were spindle shaped, whereas that of SWB1 was fairly pinching.

In the specimens with narrow slits, the top of the spandrel touched the column at large deflection angle, which initiated the increase in beam resistance. The increase in SW01 was smaller because the buckling of the spandrel reinforcement bar caused the spalling of concrete prior to compressive crushing.

CRACK PATTERNS OF SPECIMENS

The crack patterns of specimens at +3rd cycle, story deflection angle R = 1/100 rad, are shown in Fig4. The solid lines and the dotted lines indicate

the cracks due to positive and negative loading, respectively.

When the beams were deformed in bottom tension, the diagonal cracks were observed in the spandrel of SW00 due to the compressive stress. Similar cracks were observed in the specimens with narrow slits after the touch of the spandrel.

When the beams were deformed in top tension, vertical cracks were observed in the spandrel of SW00 and SW01, in which the spandrel bars were anchored into the column. The cracks in the spandrel of the other specimens developed from the boundany between the spandrel and the beam, which indicate that the deformation of the beam was restrained by the spandrel.

DEFORMATION MODES OF BEAM

The displacement meters were fixed at the points A, B and C in Fig 5, 104mm (35% of the total depth of the beam) away from the column face, in order to obtain the rotation angles of AB and BC against the column face. Considering these angles and the deflection angle of beam, the deformation pattern of the beam is decomposed into several modes.

The possible deformation modes compatible to crack patterns and the corresponding components of the beam deflection angle of the specimens SW00, SW01 and SW10 are shown in Fig 5 to 9. Some of the bolts supporting the displacement meters loosened during the tests due to large cracks or crushing of concrete. The corresponding data with less reliability are indicated by broken lines in the figures.

Bottom tension deflection

When the beam of SW00 was subjected to the bottom tension deflection, modes (b) and (d), which accompanies the shear deformation of the spandrel, occupied a substantial percentage of the deflection. The flexural shear crack of beam constituting mode (c) was observed during the 3rd cycle. The mode (c) increased with the load reversals, which corresponded to the crushing of the spandrel concrete. The mode (a) was relatively small throughout the test.

The deformation mode of the slitted specimens SW01 and SW10 at the bottom tension deflection, was significantly different from that of the monolithic specimen SW00. In SW01 and SW10, mode (a) and (b) due to the flexural and flexural-chear cracks in the beam dominated. Mode (c) in Fig9, which accompanies the deformation of the spandrel, was very small. The components of the deformation modes of the specimens SWB1, SWU1, and SWS1 were similar to those of SW01 and SW10. The spandrel of all the slitted specimens rotated like a rigid body. The truss action and the arch action as the shear resistant mechanisms were formed only within the beam, but not in the spandrel. Hence the shear strength of the slitted spandrel beam at bottom tension should be equivalent to that of the beam without the spandrel.

From the fact that the spandrel rotates like a rigid body, and assuming that the neutral axis locates at the top end of the beam and the deformation of the column and the joint is much smaller than that of the beam, the story deflection angle R at the initial contact of the spandrel to the column can be roughly estimated as follows:

$$R = \frac{(\text{width of slit})}{(\text{height of spandrel})} \times \frac{(\text{clear beam length})}{(\text{span between columns})} \qquad \text{----------(1)}$$

The calculated story deflection angles from eq (1) are compared to the observed values in Table 4. The equation (1) gives a good estimate. The observed angle at the contact in the 8th cycle is larger than that in the 6th cycle, which is attributable to the residual plastic strain in the beam bars.

Top tension deflection

When the beam of the specimens SW00 and SW01 were subjected to the top tension deflection, a substantial contribution of modes (b) (c) (d) was observed in the earlier load cycles. At the later load cycles, however, the contribution became smaller, which corresponded to the deterioration of the anchorage of the spandrel bars in the column.

When the beam of specimen SW10 was subjected to the top tension deflection, the contribution of the mode (a) was large in every load cycle. The components of the deformation modes of the specimens SWB1, SWU1 and SWS1 were similar to that of SW10, except that the mode (c), the shear deformation in the critical region, was not observed in SWB1, SWU1 and SWS1. The spandrel should have played a certain role in the shear resistant mechanism of the spandrel-beam.

DISTRIBUTION OF BEAM BAR STRAIN

The strain distribution of SWS1 and SWU1 at the peaks of the 1st cycle is shown in Figs 10 and 11. The tensile strain was observed at the compression side of the critical section of SWS1 top bar, which indicated the insufficient anchorage of the top bar within the joint. The anchorage of the bottom bar was better than that of the top bar, both in SWS1 and SWU1. The anchorage of the beam bars of SWB1 was similar to that of SWU1, whereas that of SW00, SW01 and SW10 was better. The bond stress condition of beam bars in the joint should be more critical in SWB1 than SW01 and SW10, partly because the yield strength of main bars of SWB1 was a bit larger, and partly because the yield penetration of top bars into the joint should be larger due to the restraint by the spandrel when the SWB1 beam was deformed in top tension.

COMPONENT OF STORY DISPLACEMENT

Examples of the component of story displacement are shown in Fig 12. Deformation of all the specimens except SWS1 concentrated in the beam. In the specimens SWS1, the contribution of the joint was abont 25% at 3rd cycle and was 35% at 7th cycle, which was comparable to that of the beam.

ENERGY DISSIPATING CAPACITY

Energy dissipating capacity in every half cycle is shown in Fig 13, where the half cycle is defined as the loading excurtion between zero-story-shear points. The energy dissipating capacity of SWS1 was less than one-half of that of SW10 at reversed cycles, because of the pinching hysteresis loop. It should be noted that the large deformational capacity and large energy dissipating capacity can be obtained in the slitted spandrel beam, if the depth of the column is large enough to restrain the bond deterioration of the beam bar and the shear deformation within the joint.

CONCLUSIONS

(1) Flexural strength of the slitted spandrel beam can be estimated by the ordinary plane-section analysis of the critical section.
(2) Large deformational capacity and large energy dissipating capacity are obtained in the slitted spandrel beam, if the depth of the column is large enough to restrain the bond deterioration of the beam bar and the shear deformation within the joint.
(3) The slitted spandrel contributes to the shear resistant mechanism of the spandrel beam at the top tension deflection, but not to that at the bottom tension deflection.
(4) The slitted spandrel rotates like a rigid body at the bottom tension deflection. The story deflection angle at the contact of the spandrel to the column can be roughly estimated by eq (1) in the weak girder type frame.

ACKNOWLEDGEMENTS

The authors appreciate the great contribution by Professor S. Otani of the Univ. of Tokyo, for his valuable guidances and suggestions throughout the study. Technical advises and assistances by Mr Y. Hosokawa and Mr A. Tasai of the Univ. of Tokyo, by Mr H. Kabeyazawa of Yokohama National Univ. and by the members of the Buiding Research Institute are also acknowledged.

REFERENCE

(1) " Report on the damage by 1968 Tokachi-oki earthquake," Architectural Institute of Japan, 1968
(2) " AIJ Standard for Structural Calculation of Reinforced Concrete Structures," Architectural Institute of Japan, 1981

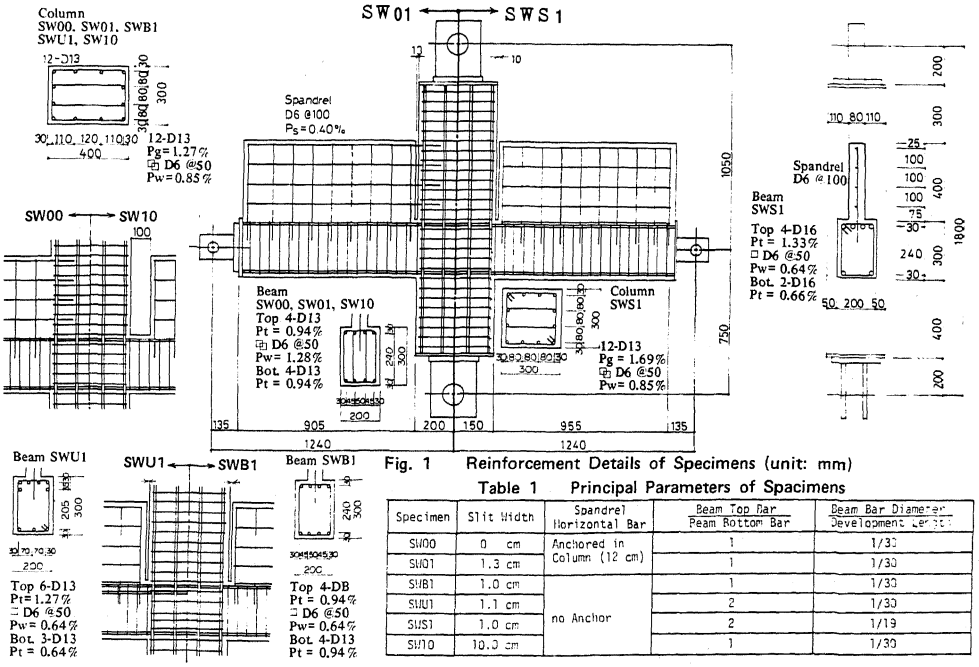

Fig. 1 Reinforcement Details of Specimens (unit: mm)

Table 1 Principal Parameters of Specimens

Specimen	Slit Width	Spandrel Horizontal Bar	Beam Top Bar / Beam Bottom Bar	Beam Bar Diameter / Development Length
SW00	0 cm	Anchored in Column (12 cm)	1	1/30
SW01	1.3 cm		1	1/30
SWB1	1.0 cm	no Anchor	1	1/30
SWU1	1.1 cm		2	1/30
SWS1	1.0 cm		2	1/19
SW10	10.0 cm		1	1/30

Table 2 Properties of Concrete

Properties \ Specimens	SW00, SW01, SW10 (60 days)	SWB1, SWU1, SWS1 (22,26 & 29 days)
Secant Modulus	240 t/cm²	188 t/cm²
Compressive Strength : Fc	0.278 t/cm²	0.250 t/cm²
Strain at = Fc	0.00280	0.00220
Descencing Stiffness after Fc	- 25 t/cm²	- 28 t/cm²
Splitting Tensile Strength	0.024 t/cm²	0.021 t/cm²

Table 3 Properties of Reinforcing Bars

(a) Specimen SW00, SW01 and SW10

	D13	D6
Yield Stress : σ_y	3.37 t/cm²	3.77 t/cm²
End of Yield Plateau : ε_{SH}	23.5 x 10^{-3}	No Plateau
Tensile Strength : σ_M	5.05 t/cm²	4.93 t/cm²

(b) Specimen SWB1, SWU1 and SWS1

	D16	D13	D6
Yield Stress : σ_y	3.92 t/cm²	3.74 t/cm²	3.69 t/cm²
End of Yield Plateau : ε_{SH}	0.0180	0.0220	0.0211
Tensile Strength : σ_M	5.56 t/cm²	5.50 t/cm²	5.06 t/cm²

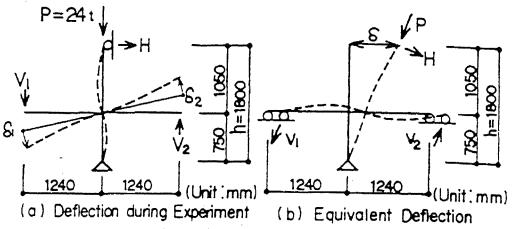

(a) Deflection during Experiment (b) Equivalent Deflection

Fig.2 Loading procedure

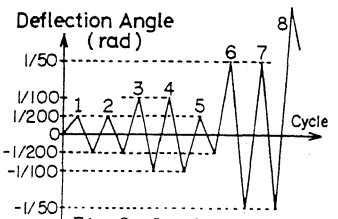

Fig.3 Loading history

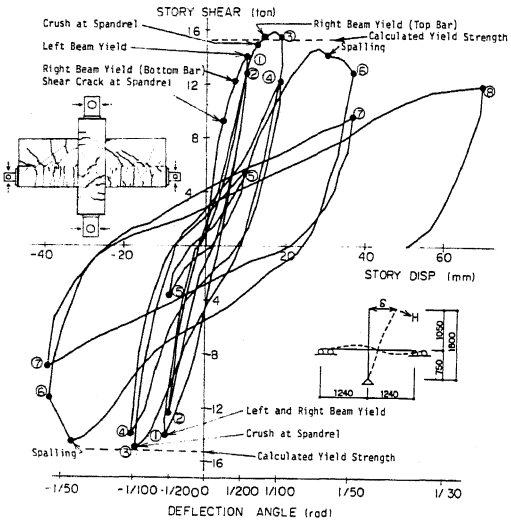

(a) Specimen SW00

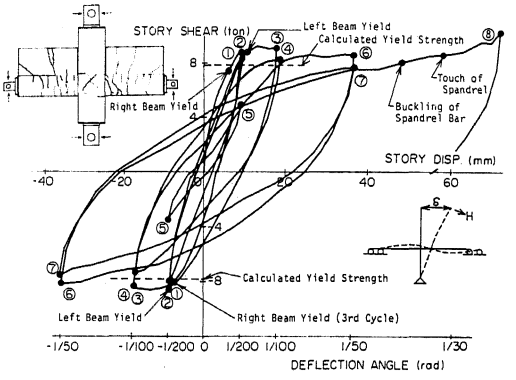

(b) Specimen SW01

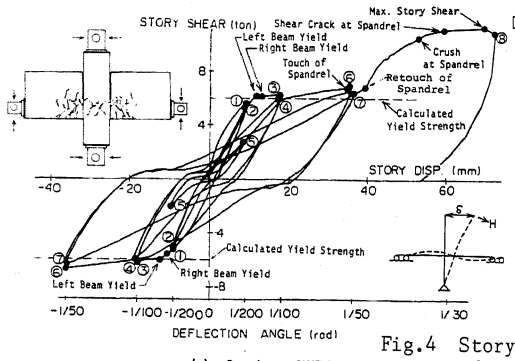

(c) Specimen SWB1

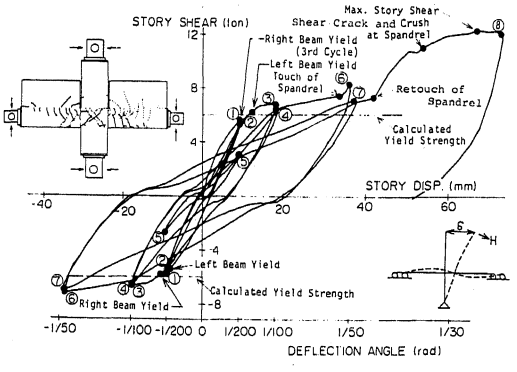

(d) Specimen SWU1

Fig.4 Story shear - story displacement relationships and crack patterns (at +3rd cycle, R=1/100rad)

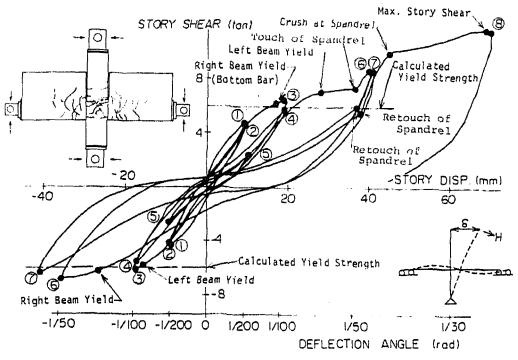

(e) Specimen SWS1

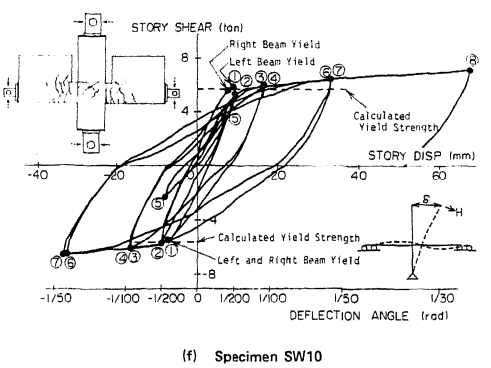

(f) Specimen SW10

Fig.4 Story shear - story displacement relationships and crack patterns (at +3rd cycle, R=1/100rad)

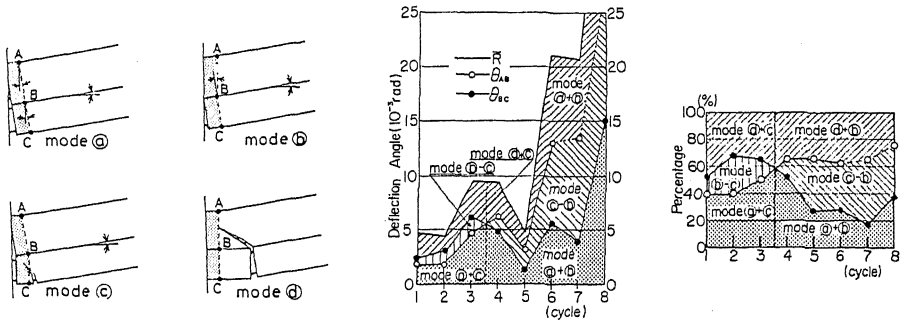

Fig.5 Deformation modes of SW00 beam (bottom in tension)

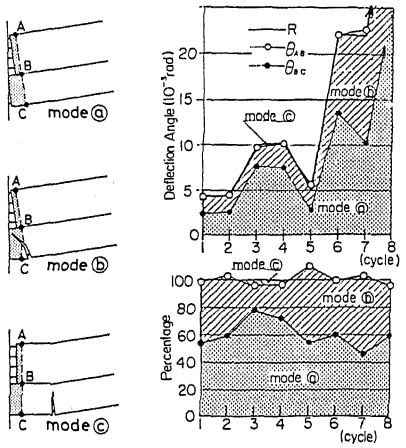

Fig.6 Deformation modes of SW01 beam (bottom in tension)

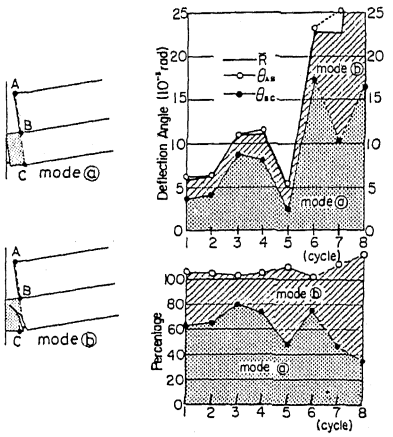

Fig.7 Deformation modes of SW10 beam (bottom in tension)

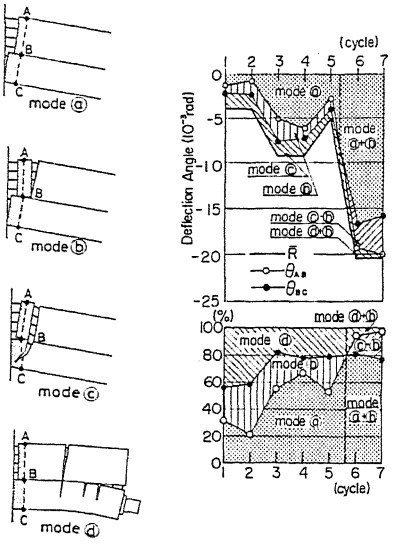

Fig.8 Deformation modes of SW01 beam (top in tension)

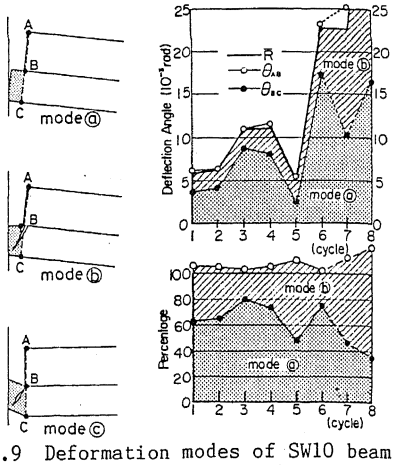

Fig.9 Deformation modes of SW10 beam (top in tension)

Table 4 Story deflection angle at the contact of the spandrel to the column

		SW01	SWB1	SWU1	SWS1
Observed story deflection angle	6th cycle	Not touch	19.3×10^{-3}	18.7×10^{-3}	19.9×10^{-3}
	7th cycle	Not touch	Not touch	Not touch	20.2×10^{-3}
	8th cycle	31.8×10^{-3}	22.6×10^{-3}	23.6×10^{-3}	20.7×10^{-3}
Calculated by eq (1)		22.7×10^{-3}	20.9×10^{-3}	20.6×10^{-3}	22.0×10^{-3}

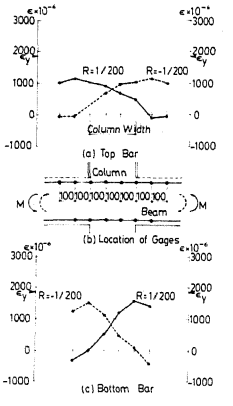

Fig.10 Steel strain distribution of SWS1

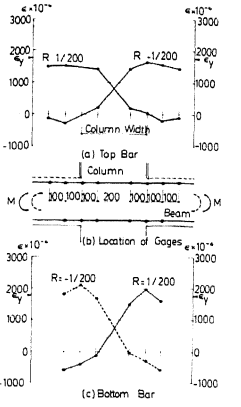

Fig.11 Steel strain distribution of SWU1

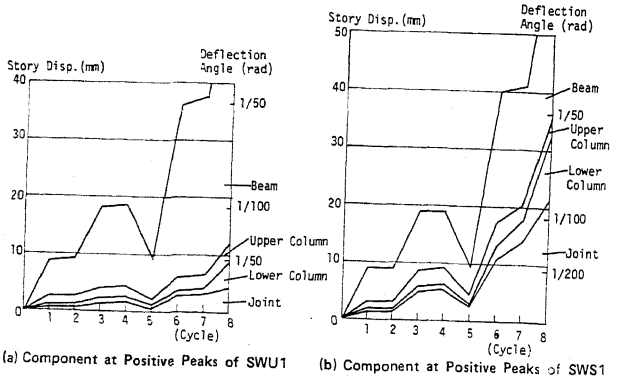

Fig.12 Component of story displacement

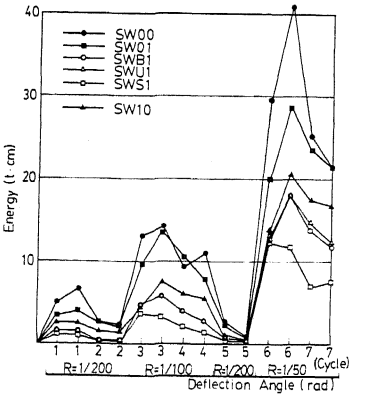

Fig.13 Energy dissipation in every half cycle